American Mineralogist, Volume 69, pages 139–153, 1984

Symplectic exsolution in olivine

DAVID MOSELEY[1]

Department of Geology
University of Manchester
Oxford Road, Manchester M13 9PL, England

Abstract

Intergrowths of augite and magnetite (type A symplectites) have been examined in eight olivines ranging in composition from Fo_{86} to fayalite. For Fo_{86} the Mg/Fe ratio in the exsolved pyroxene is the same as that of the olivine matrix. In more fayalitic compositions the pyroxene is enriched in Mg relative to the olivine matrix.

For olivines of plutonic origin two structural orientations between clinopyroxene and host have been observed. They are related by a 60° rotation about $[100]_{ol}$. Magnetite forms only one orientation relationship with olivine, but because of its high symmetry, magnetite–augite lattice orientations are always the same. These symplectites are plate-like lying on $(100)_{ol}$, with a tendency to be elongated along $\langle 010\rangle_{ol}$ or $\langle 013\rangle_{ol}$; directions that are pseudosymmetrically related. For both pyroxene orientations the common habit plane is $(100)_{ol}\|(100)_{px}\|(1\bar{1}1)_{mt}$. There is evidence to suggest that magnetite can start to form before pyroxene. It is possible that both pyroxene and magnetite grow into the olivine by the propagation of ledges along their interface with the host phase.

It is suggested that the formation of these intergrowths is caused by the presence of ferric iron in the olivine. On cooling the olivine structure eventually contracts to a critical size below which the electrostatic repulsion between Fe^{3+} and Si^{4+} becomes too great for stability. This initiates a reaction which can be summarized by the equation:

$$3Fe^{3+}_{4/3}\square_{1/3}SiO_4 + Fe^{2+}_2SiO_4 + 4X_2SiO_4 \rightarrow 2Fe_3O_4 + 4X_2Si_2O_6$$

where X = Ca, Mg, Fe. The pyroxene phase acts as a sink for elements not compatible with the olivine structure, such as Al and Ca. Augite is formed as long as there is sufficient Ca present and the temperature is high enough for it to diffuse to the reaction sites. Exhaustion of Ca or a drop in temperature can lead to the spinel–two pyroxene assemblages reported in some earlier studies.

Introduction

Over the past few years there has been some debate on the origins of the microscopic intergrowths of spinel and pyroxene, known as symplectites, that are found in or are associated with some olivines. Bell *et al.* (1975) have described six different types (A to F) and attributed them to one of four origins. (The term symplectite is, of course, simply a useful appellation for certain types of worm-like intergrowths and is of no genetic significance.) The work by Bell *et al.* was, in part, based on an earlier study by Gooley *et al.* (1974). Both these studies were of lunar material, on which much of the recent olivine symplectite work has been done. Terrestrial occurrences have tended to receive less attention, though new examples are still reported along with discussions of their probable origins, *e.g.*, a type A from the Japanese alpine peridotite (Arai, 1978) and a type C from a layered, basic intrustion in Australia (Ambler and Ashley, 1977). This report deals with an additional eight terrestrial examples which have been studied by electron microscopic techniques as well as the more usual microprobe and optical methods.

The olivines used in this work were a Fo_{86} (specimen 199) and a Fo_{81} (RH9) from unit B of the Western Layered Series and unit 10 of the Eastern Layered Series, respectively, of the Rhum pluton, Scotland. Also from Scotland was a Fo_{72} (SK28) collected from the Cuillin Complex, Isle of Skye. A Fo_{53} (Specimen 9898) from the Onverwacht dunite pipe in the Bushveld complex, three specimens, Fe_{32}, Fo_{28}, Fo_3 (nos. 4130, 4308, 4472, respectively) from the Skaergaard intrusion and a pure fayalite (RPT) from Rockport, Massachusetts, were also examined. The specimens (Fig. 1) are similar to the type A of Bell *et al.* (1975). However, in this study in the six specimens for which the spinel phase has been analyzed it

[1] Present address: Department of Physics, University of Warwick, Coventry CV4 7AL, England.

0003–004X/84/0102–0139$02.00

was found to be magnetite and not chromite as in the symplectites examined by Bell *et al.* The symplectites are plate-like, approximately rectangular in shape with a thickness varying from about 0.05 to 0.5 μm. They vary from about 1 μm to more than 100 μm in length, though typically they are about 25 μm long and about 0.2 μm thick (Figs. 1 and 2).

This particular type of symplectite was reported at least as early as 1871 by Zirkel. Through these and subsequent sporadic accounts it has become sufficiently well known to be illustrated in student text books (*e.g.*, Harker, 1954 and Hatch *et al.*, 1972). However, no comprehensive description of it has ever been given, nor, until about ten years ago, were there any serious attempts to account for its origin, though Judd (1885) tried to explain the development of these intergrowths from an examination of a series of specimens from the Scottish Hebrides which had formed at different depths. Recent interpretations of the formation of type A symplectites include the breakdown of garnet inclusions, exsolution (Bell *et al.*, 1975), oxidation and cellular decomposition (Putnis, 1979).

The abundance of these intergrowths varies from being so rare that they may be overlooked in an optical thin section (4308, 4310) to densities high enough to render the host olivine opaque and give it the appearance of magnetite (4472). The apparent concentrations of these symplectites are misleading. Even in the "opaque" olivine their volume fraction is less than five percent. More usual symplectite concentrations are about that exhibited by the Bushveld specimen (Fig. 1a) which is less than one volume percent. Single-crystal X-ray studies both by oscillation and rotation photography about the *a*-, *b*- and *c* axes were made of specimens 199, 9898 and RPT. Exposures of up to four days failed to produce any spots which could not be attributed to olivine. Except in sections approximately perpendicular to (100), ion-thinned samples of these specimens were not observed to contain any symplectites, even though a dozen or more symplectites might have been visible in the pre-thinned samples (which were 1 mm in diameter and 30 μm thick). Low symplectite volume-fractions in olivines which appeared to contain high concentrations of these intergrowths were also reported by Bell *et al.* (1975) who investigated the effect in some detail. They concluded that the average volume occupied by type A symplectites, in their samples is seldom more than one volume percent and is "generally about 0.5 vol.%". The highest density they observed was 1.3 volume percent.

Optical petrography

Type A symplectites are intergrowths of spinel and pyroxene. However, they are so thin that the difference in optical properties between pyroxene and olivine is, in general, insufficient for the pyroxene phase to be observed. Early reports noted only the spinel (*e.g.*, Judd, 1885; Harker, 1954). The magnetite, when viewed at high magnifications, is often reddened, and it would appear that dark red is the characteristic color of this mineral when less than a micron thick, as ultra-thin sections of magnetite crystals prepared for electron-optical studies have also been observed to be reddish. (P. P. K. Smith, pers. comm.).

The symplectites, in the olivines used in this investigation, are invariably absent near grain edges (Fig.1a), and smaller symplectite-free zones can occur within a crystal. Figure 1b shows what appears to be two symplectite generations; an earlier one comprising large individuals in a diagonal band across the figure and a later phase of smaller growths which are not present near the larger ones. Examination of a large number of grains showed that these type A symplectites generally form on the (100) olivine planes and are elongated in one of three preferred directions which are inclined at 120° to each other. They correspond to the ⟨010⟩ and the two ⟨013⟩ directions of the olivine host. This is most obvious in the Bushveld sample where strong (010) cleavage traces are also present (Fig. 1b–d). Symplectite detail is shown in Figure 1c and d in which it can be seen that branching within individual intergrowths also tends to be along these directions, though this is less pronounced in one of the samples (199) from Rhum where branches additionally form along ⟨001⟩. A further feature, observed particularly in the Bushveld specimen, is that the ⟨010⟩ symplectites are narrower and more numerous than the ⟨013⟩ types (Fig. 1b–d). These differences in the two types are less pronounced in other samples.

Although the larger symplectites often appear to have random orientations, this is an optical effect. Observations at higher magnifications show that the large symplectites in Figure 1b are the normal ⟨010⟩ and ⟨013⟩ types. That at A, for example, is an ⟨010⟩ type with natural edges showing at left and on top, while the diagonal edge is a truncation by one face of the thin section because the (100) plane (on which these intergrowths lie) is slightly inclined to that of the section. The more common case is where both ends of the symplectite have been cut off by the top and bottom of the thin section, giving rectangular shapes such as that at B in Figure 1b. This leads to all large symplectites in the same grain having the same apparent orientations which, in general are non-crystallographic. A fact which appears to have been overlooked in some previous studies.

Occasional symplectites are found with magnetite cores. In the ones so far observed these cores tend to have rectangular shapes which are elongated along [010] of olivine. Isolated examples of these symplectites can be seen in Figure 1c and d, while a group of them are shown in Figure 1e. The branching in this variety of type A symplectite, like those without magnetite cores, shows a preference for ⟨010⟩ and ⟨013⟩ directions. Another slightly different type is found in the Rockport fayalite in which orientation relationships do not conform with the simple scheme found in all the other specimens. In addition to

the more common elongated type, a smaller, apparently elliptical, type is also observed on the (001) as well as the (100) plane (Fig. 1f). The elliptical appearance is to some extent a depth of focus effect on symplectites which are inclined to the plane of the thin section. These intergrowths possibly show early stages in the normal development of this type of symplectite and are the ones in which the pyroxene phase is most readily visible.

Bell *et al.* (1975) reported that some of their type A symplectites had small hollow cores: none of the ones so

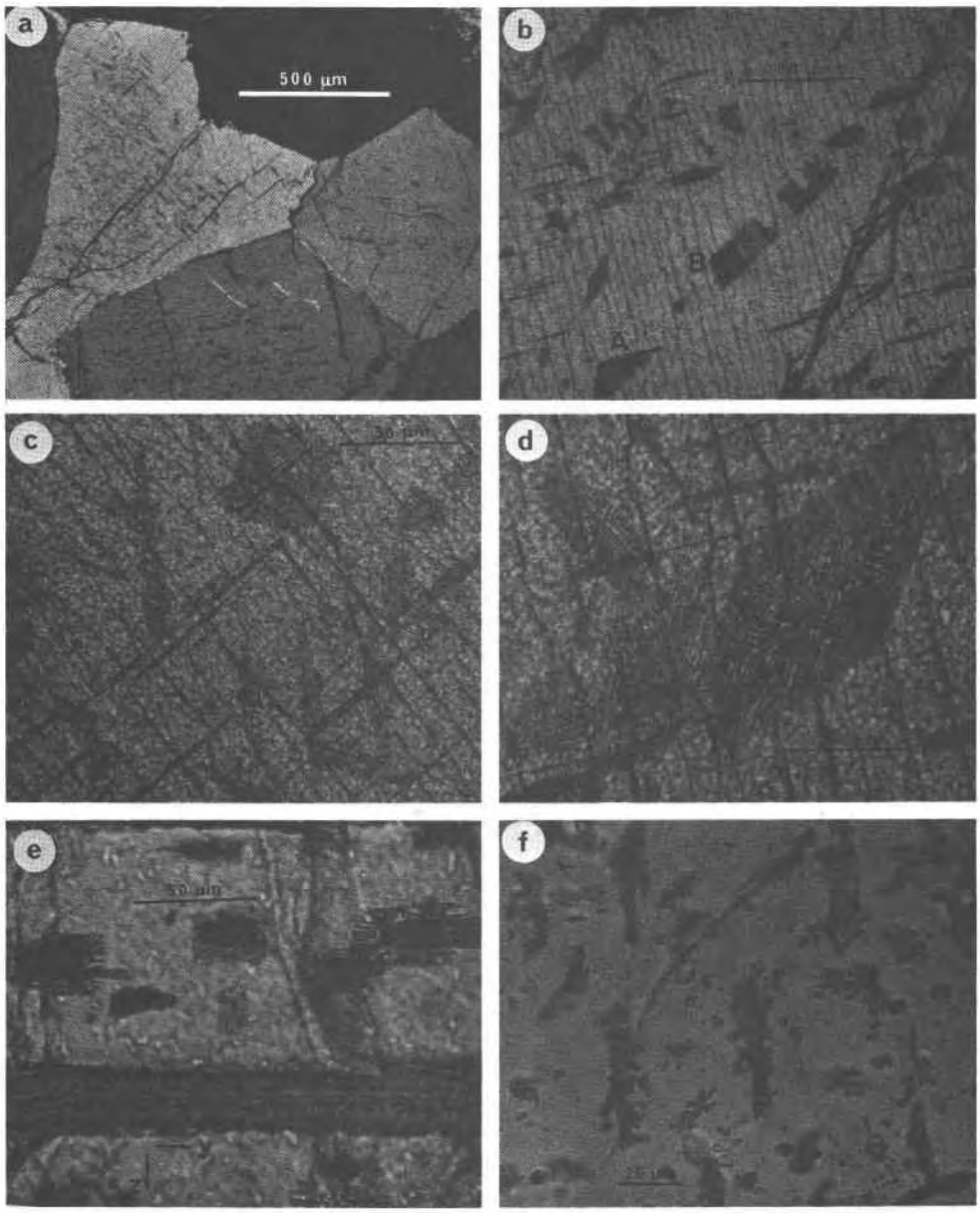

Fig. 1. Optical micrographs of type A symplectites. (a) General view showing symplectites in more than one orientation and absent near grain boundaries. (b)–(d) Detail on an almost (100) section with prominent (010) cleavage. Diagonal band across (b) is thought to be earliest generation of symplectites on a (100) plane truncated by the faces of the rock slice. Note the absence of smaller symplectites near this band. (c) Characteristic elongation of symplectites in three directions. (d) Detail showing that the branching in individual symplectites is also preferentially along $\langle 010\rangle_{ol}$ and $\langle 013\rangle_{ol}$. (e) A group of symplectites with magnetite cores (the band parallel to y is serpentine). (f) Two generations (?) of symplectites. Elongate (out of focus) set seems to lie on (001) while the smaller (embryo) set is on (100). View is about 3° from [512]. Micrograph (a) was taken in crossed polarized light, the others in plane polarized light. (a)–(d) Bushveld, (e) Rhum (199) and (f) Rockport.

far observed in this study have been found to have this characteristic.

Electron petrography

Ion-thinned foils of all eight specimens were examined with a Philips 301 electron microscope. In general sections approximately parallel to [100] were used since only these orientations were found to contain symplectites in the finished sample. Because of this the symplectites are seen approximately edge on and have a lamellar-like appearance in electron micrographs. Generally the platelets have straight, parallel sides, as shown in Figure 2a, and (in conformity with the optical studies) interfaces parallel to (100) olivine. Exceptions to this are some

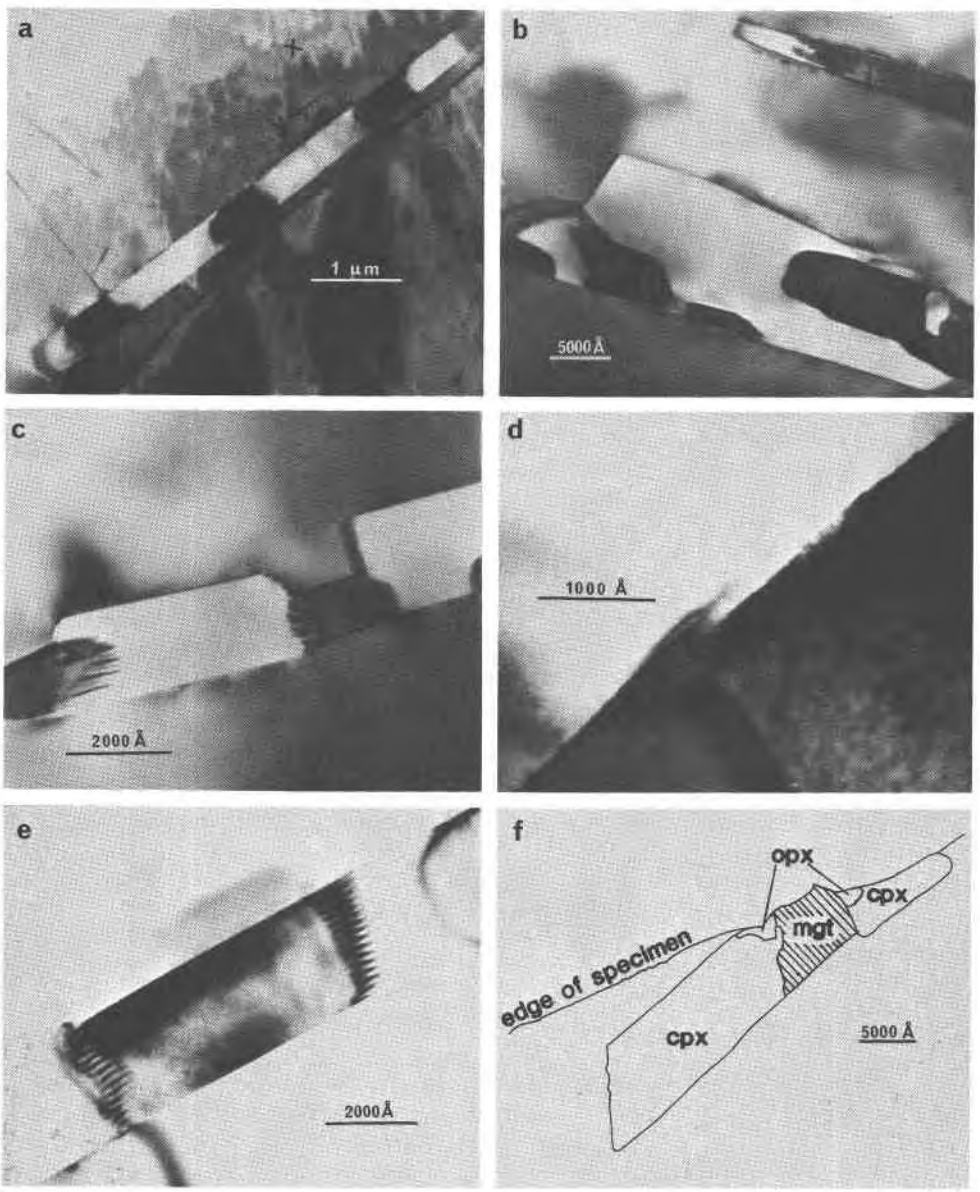

Fig. 2. Electron micrographs of type A symplectites. (a) Edge-on view of a typical platelet. (b) and (c) some of the less regular shapes observed in a specimen with high symplectite densities. (d) Detail of an interface with step-like features between magnetite (right) and pyroxene and olivine matrix. Note that the pyroxene steps are smaller than those of the magnetite and that this phase appears to have partially overgrown the magnetite. (e) Detail of a pyroxene-magnetite interface with dislocations. (f) Sketch, from a micrograph, of a complex symplectite. In all micrographs magnetite is the darker phase. (a), (d) and (e) Bushveld, (b) and (c) Skaergaard (4472) and (f) Rockport.

symplectites observed in specimen 4472 (*e.g.*, Figs. 2b and c) which has a high density of these intergrowths. Some of the irregular shapes in this sample are possibly formed by two, or more, symplectites coalescing during growth, or are the result of pyroxene apparently still being exsolved after the precipitation of the magnetite phase was complete (Figs. 2c and d).

Both the pyroxene and the magnetite often have interfaces with the olivine that are stepped (Fig. 2d) on the $(100)_{ol}$ planes. The steps between the magnetite and the olivine host are higher than those associated with pyroxene, *i.e.*, about 40Å compared with about 10Å. These steps are of a fairly uniform length, about 150 to 200Å, with those of the pyroxene a little shorter, on average, than those in the magnetite. The visibility of these steps seems to be dependent on the orientation of the symplectite and shows up best when the electron beam is parallel to the *c*-axis of the pyroxene. The interface between the magnetite and the pyroxene, although approximately perpendicular to $(100)_{ol}$, is irregular and contains dislocations (Fig. 2e), as do the interfaces between symplectic phases and olivine.

The curious mottling effect in the magnetite phase (best seen in Fig. 2d) is characteristic and has also been observed by Smith (1979) in magnetite minerals. He considered it to be an artifact introduced in the ion thinning process as he found it to be absent in grains prepared by crushing.

Diffraction studies of the igneous samples show that, with respect to the olivine, there are two structural orientations of the pyroxene, which can be indexed as augite (*C2/c*), and one of magnetite (Table 1). Diffraction patterns and their interpretations are given in Figure 3 for magnetite and both pyroxene orientations. From Table 1 it can be deduced that the Si chains in the pyroxene (which lie along c_{px}) are formed parallel to either $\langle 010\rangle_{ol}$ or $\langle 013\rangle_{ol}$, the same directions along which the symplectites were observed to be elongate in the optical studies. Because of the approximately hexagonal close-packing of oxygen ions in olivine, $\langle 010\rangle_{ol}$ and $\langle 013\rangle_{ol}$ are structurally similar and, in the ideal structure, would be exactly 60° apart. Further deductions which can be made from Table 1 are that the approximately close-packed oxygen layers of olivine and magnetite are parallel and that all the $\langle 010\rangle$ and $\langle 013\rangle$ directions in olivine are parallel to a $\langle 112\rangle$ direction in magnetite.

Table 1. Structural orientations between host olivine and symplectitic phases

olivine		magnetite		augite†				
(100)*	//	{111}	//	(100)	or	(100)	or	(100)
[010]	//	<112>	//	[001]		[011]		[01$\bar{1}$]
[001]	//	<110>	//	[010]		[01$\bar{3}$]		[013]

*Interfacial plane on which symplectites form.

†Only one augite orientation was observed in any given symplectite. However, more than one orientation can be present in different symplectites from the same sample.

Structural relationships in the Rockport fayalite are more complex: optical studies suggest that symplectites are apparently present on (001) as well as (100) olivine planes. Electron optical studies indicate that while the pyroxene and magnetite phases on the (100) planes have the same orientations with each other and the host phase as in all the other samples, the intergrowths on the (001) planes appear to have developed with little structural control from the olivine. No magnetite orientation with respect to olivine has obtained for this latter set and the only clinopyroxene orientation to have been established unambiguously is $[100]_{ol}\| \sim [011]_{cpx}$, $[010]_{ol}\|[201]_{cpx}$ (which is $\sim a^*_{cpx}$) and $[001]_{ol}\| \sim [0\ 3\ \bar{1}0]_{cpx}$. The interface between this symplectite and its host could not be determined, thus it is not certain that the second set of symplectites are exsolved exactly on $(001)_{ol}$. Associated with some clinopyroxene diffraction patterns in this specimen are fainter spots indicating a second phase with larger cell parameters. These were also observed with a hedenbergite for which the structural relationship with olivine was obtained. In this case (Fig. 2f) the second phase could be indexed as an orthopyroxene (*Pbca*) with $(100)_{cpx}\|(001)_{opx}$, $[010]_{cpx} \perp (110)_{opx}$, $[001]_{cpx}\|[\bar{1}10]_{opx}$(or $[100]_{ol}\|[010]_{opx}$, $[010]_{ol}\|[001]_{opx}$, $[001]_{ol}\|[100]_{opx}$). Since the Rockport fayalite differs little in composition from specimen 4472 (Fo3) it could be that geological rather than chemical factors are responsible for the additional symplectite orientations in this fayalite. The description by Penfield and Forbes (1896) of the original locality of this fayalite suggests that it had a skarn-like (metamorphic) origin. If this is the case then some of these symplectites may have nucleated during heating, rather than cooling as for the other olivines.

Analytical procedures

Table 2 gives microprobe analyses[2] of the olivines used in this work and, where present, coexisting primary crystals of augite and spinel. Every tabled probe analysis is of a single spot, chosen as being closest to the average of all the determinations for that mineral. Variations from these values greater than ±1.5 mole% in the recalculated analyses were not observed, except as noted below. Generally the variation was less than 1 mole%.

For olivines, between twelve and twenty analyses were made for each specimen. Specimen 4472 showed some variation in its Ca and Mg contents, possibly because of its high symplectite density. A 4 mole% increase in forsterite content was found near the more aluminous spinels in specimen 9898. (This was attributed to oxidation of the olivine in these areas as they are also

[2] All microprobe analyses were performed on a Cambridge Instruments Geoscan fitted with a Link System Model 290-2KX energy-dispersive spectrometer.

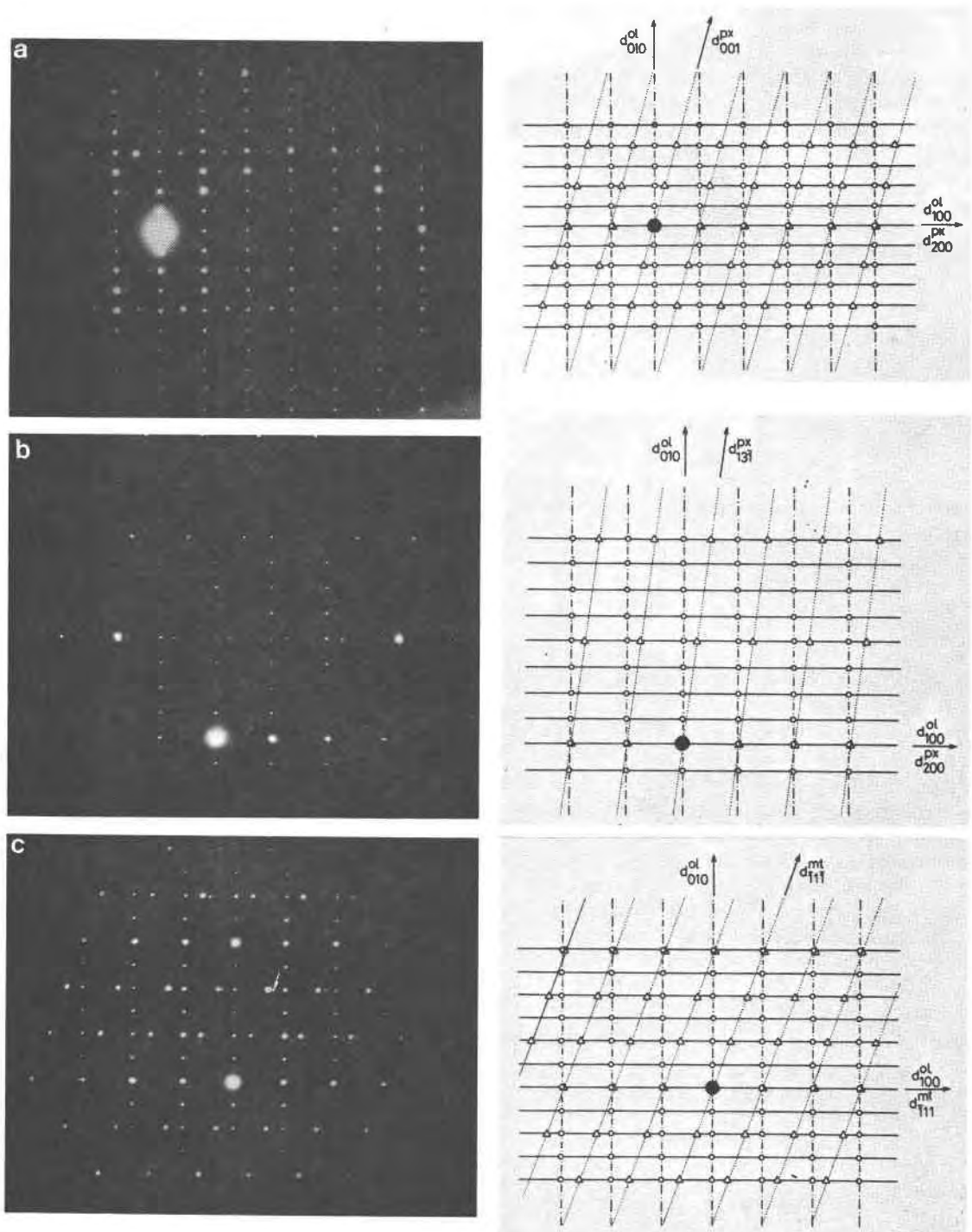

Fig. 3. Diffraction patterns and their interpretations. (a) and (b) olivine and pyroxene, (c) olivine and magnetite, with $[001]_{ol}$ parallel to: (a) $[010]_{px}$, (b) $[013]_{px}$ and (c) $[110]_{mt}$. The fainter spots in (c), such as the one arrowed, are from the augite phase. (a) is from specimen 4308, (b) and (c) are from 9898.

reddened near these spinels.) A smaller variation due to zoning from core to edge was also detected in this specimen. All the other specimens were, within analytical error, compositionally homogeneous. The individual crystals of augite and spinel were not examined in as much detail. Usually only four to six analyses of each mineral was made. Like the olivines they do not appear to vary much either from core to margin or from grain to grain.

The olivines and their symplectite inclusions were also exam-

ined with an analytical electron microscope (EMMA-4[3]). Table 3 gives matrix, pyroxene and spinel analyses of six of the samples. For the seventh, specimen 4310, olivine and pyroxene only are given, as all but a small fragment of the symplectite had been eroded away during the ion thinning. In the eighth specimen (RH9) the symplectites are too small (about 1 μm by 0.05 μm) for chemical analysis. The augite composition is listed in Table 3 for this sample, is from a pyroxene inclusion which may be part of a larger symplectite but it could also be connected with another, unrelated phenomenon.

Under ideal conditions spots 0.1 μm in diameter can be analysed in the EMMA-4, and symplectites, which are usually about 0.2 μm across, are in principle well within its capability. Specimens cannot, however, be tilted within this microscope. Consequently for thin foils with sections which are not almost perpendicular to $(100)_{ol}$ the inclination of the symplectite to the electron beam can be sufficient that part of the beam travels through olivine host near one (or both) edge(s) of the specimen. This problem is more severe for the volumetrically smaller magnetite phase; analyses of which not uncommonly showed contamination by both olivine and pyroxene. This contamination causes greater analytical variations than were observed in the microprobe results. However, uncontaminated analyses, such as those of matrix olivine away from symplectites, exhibited variations of less than ±2 mole%. Only slightly greater than the variation in the microprobe results.

The augite analyses given in Table 3 are those with the highest Ca content since these should be the analyses least contaminated by olivine. In general it was found that the higher the Ca content, the greater was the deviation between the Mg/Fe ratios in pyroxene and host, and also when recalculated on the basis of O = 6, the sum of the Si and Al cations increased with increasing Ca content. The magnetite analyses given in Table 3 are those with the lowest Si contents, but where circumstances permit, augite and magnetite analyses are from the same symplectite even though these may not be the "best" analyses. In all cases the olivine analysis is one taken in the vicinity of the given pyroxene analysis. Al in areas well away from symplectites was always below the limit of detection in the matrix. Occasionally, however, it was present near one of these intergrowths, as for example, in 4308. Although the two sets of olivine analyses given in Table 2 and 3 show some differences, this is without significance. The maximum difference (specimen 4310) is only 3 mole% and there is sufficient analytical variation in both the EMMA-4 and microprobe analyses for the ranges of values obtained by the two methods to overlap.

Within the limits of analytical error, and allowing for contamination from other phases, there seemed to be no compositional variation for either the magnetite or, with two exceptions, the pyroxene in different symplectites from the same specimen. The exceptions were a symplectite in specimen 199 (Fo_{86}) and one in specimen 4308 (Fo_{28}), in both of which low Ca-pyroxene at one end changed to high Ca-pyroxene over a distance of about 0.5 μm. This effect could not be checked at the other end of either symplectite because, in one case the far end of the symplectite lay in an area too thick for analyses and in the other it had been removed during ion-thinning. The better of the two sets of analyses showing this change is given in Table 4. Unfortunately the numerous analyses required to establish the change in pyroxene composition distorted it too much for subsequent diffraction studies, so that the structure of the low Ca-pyroxene is unknown.

[3] EMMA is an AEI-EM802 electron microscope modified to take a KEVEX solid-state energy-dispersive detector.

Discussion of results

The structural orientations of symplectic phases which are presented in Table 1 are consistent with the optical observations. Combining optical and electron microscopic results, a detailed scheme of symplectic development can be inferred. In the slowly cooled igneous specimens, symplectites form on the close-packed (100) planes of olivine. Close-packed $(111)_{mt}$ planes are parallel to them and the magnetite apparently has a preference for growth along its $\langle 112 \rangle$ directions on this plane when exsolved in olivine. The $\langle 112 \rangle_{mt}$ are parallel to $\langle 010 \rangle_{ol}$ and $\langle 013 \rangle_{ol}$; the three directions along which the symplectites are found to be preferentially elongated. These directions are also those along which $[001]_{px}$ can lie. Although no direct evidence is available, it seems reasonable to suggest that symplectites are elongated parallel to the *c*-axis of their pyroxene phase; this, being the direction along which the $[SiO_3]_n$ chains form, is the preferred growth direction of these silicates. The step-like features, such as shown in Figure 2d can be interpreted as growth ledges, analogous to those described by Champness and Lorimer (1974) on the interface of exsolved augite lamellae in orthopyroxene. Since the ledges appear to propagate along $[010]_{px}$, this would seem to conflict with the suggestion that the growth direction is parallel to $[001]_{px}$. However, this can be reconciled if the transformation along $[001]_{px}$ is rapid as this could lead to a stepped profile normal to the $[001]_{px}$ direction. This interpretation is illustrated schematically in Figure 4, which shows how a profile, such as that in Figure 2d might develop. (Unfortunately, because of the difficulties in preparing $(100)_{ol}$ samples containing symplectites, it has not been possible to verify this suggestion.) A detailed scheme for this suggested transformation of olivine to pyroxene along $[010]_{ol}$ with the structural orientation determined by electron diffraction is shown in Figure 5. It indicates that this transformation could take place quite readily with minimal diffusion and structural alterations. The olivine–pyroxene transition along $\langle 013 \rangle_{ol}$ is similar.

The fact that some symplectites have magnetite cores suggests that magnetite can be the first phase to precipitate. As many electron micrographs indicate that pyroxene continued to grow after magnetite formation had ceased, it is possible that magnetite is normally the first phase to precipitate. If this is so then symplectites may develop as shown in Figure 6. In this scheme magnetite nucleates and starts growing more or less equally along the structurally similar directions of $\langle 010 \rangle_{ol}$ and $\langle 013 \rangle_{ol}$. Subsequent nucleation and growth of the pyroxene determines the final shape of the symplectite as cooperative growth between $\langle 001 \rangle_{px}$ and a parallel set of $\langle 112 \rangle_{mt}$ dominates the structural development. Although structur-

Table 2. Representative microprobe analyses of olivine and coexisting grains of augite and spinel

	199 (Rhum)			RH9 (Rhum)			SK28 (Skye)			9898 (Bushveld)		
	olivine	augite	spinel	olivine	augite	spinel	olivine	augite	spinel	olivine	spinel[c]	spinel[d]
SiO_2	40.19	51.00	0.00	39.29	51.64	0.35	38.03	51.56	0.43	36.61	0.24	0.24
Al_2O_3	0.00[b]	3.10	17.94	0.00	2.99	0.00	0.00	2.13	1.23	0.00	3.81	0.21
CaO	0.16[b]	23.00	0.00	0.13	21.81	0.17	0.00	21.64	0.00	0.00	0.00	0.00
MgO	46.35	15.89	11.14	43.09	16.56	0.48	36.57	16.03	0.00	25.72	1.42	0.00
FeO[a]	12.80	4.13	33.00	17.08	5.13	91.19	25.47	7.56	86.09	37.12	62.79	91.50
MnO	0.00	0.00	0.53	0.35	0.32	0.00	0.32	0.00	0.56	0.38	0.34	0.00
NiO	0.27	0.00	0.00	0.00	0.00	0.62	0.00	0.00	0.00	n.a.	n.a.	n.a.
TiO_2	0.00	1.21	1.88	0.00	0.41	0.30	0.00	0.52	6.40	0.00	13.95	1.17
Cr_2O_3	0.00	0.89	34.88	0.00	0.88	0.00	0.00	0.00	1.33	n.a.	n.a.	0.00
Total	99.77	99.22	99.37	99.94	99.74	93.12	100.38	99.43	96.04	99.83	94.58	93.12
Cations	O = 4	O = 6	O = 4	O = 4	O = 6	O = 4	O = 4	O = 6	O = 4	O = 4	O = 4	O = 4
Si	1.002	1.888	-	0.998	1.903	0.013	1.000	1.921	0.016	1.025	0.008	0.009
Al	-	0.136	0.664	-	0.130	-	-	0.093	0.053	-	0.159	0.009
Ca	0.005	0.913	-	0.004	0.861	0.007	-	0.864	-	-	-	-
Mg	1.722	0.877	0.522	1.631	0.910	0.027	1.434	0.891	-	1.073	0.075	-
Fe^{2+}	0.267	0.128	0.442	0.363	0.159	0.936	0.560	0.236	0.905	0.869	0.726	0.979
Fe^{3+}	-	-	0.426	-	-	1.978	-	-	1.719	-	1.128	1.948
Mn	-	-	0.014	0.008	0.011	-	0.007	-	0.017	0.009	0.010	-
Ni	0.006	-	-	-	-	0.019	-	-	-	-	-	-
Ti	-	0.034	0.044	-	0.012	0.009	-	0.015	0.174	-	0.370	0.034
Cr	-	0.027	0.866	-	0.026	-	-	-	0.038	-	0.335	-
Mole percent												
Ca	0.3	47.6		0.2	44.4		0.0	43.4		0.0		
Mg	86.4	45.7		81.3	46.9		71.7	44.8		55.0		
Fe	13.4	6.7		18.1	8.2		28.0	11.9		44.5		
Mn	0.0	0.0		0.4	0.6		0.3	0.0		0.5		
Mg/(Mg+Fe)	0.866	0.873		0.818	0.851		0.719	0.791		0.553		

a All Fe *given as* FeO, *but proportioned into* Fe^{2+} *and* Fe^{3+} *in the recalculated spinel analyses.*
b CaO *is not present in all analyses.*
c Large interstitial grains sometimes enclosing olivines.

Table 3. EMMA analyses of exsolved symplectitic phases and olivine host

	199 (Rhum)			RH9 (Rhum)		SK28 (Skye)			9898 (Bushveld)		
	olivine	augite	spinel	olivine	augite[b]	olivine	augite	spinel	olivine	augite	spinel
SiO_2	40.22	53.99	1.34	40.39	52.25	38.43	54.40	14.24	36.90	52.68	3.93
Al_2O_3	0.00	4.92	0.68	0.00	3.12	0.00	0.00	0.00	0.00	0.00	0.00
CaO	0.20	21.15	0.00	0.00	22.52	0.00	21.77	0.00	0.00	24.11	0.00
MgO	45.92	15.32	2.38	42.22	15.54	36.61	17.77	8.68	24.30	15.30	0.00
FeO[c]	13.37	4.52	93.02	17.19	5.67	24.96	6.06	77.08	38.31	7.91	96.07
MnO	0.18	0.10	0.00	0.20	0.00	0.00	0.00	0.00	0.49	0.00	0.00
NiO	0.12	0.00	0.00	0.00	0.00	0.00	0.00	0.00	0.00	0.00	0.00
TiO_2	0.00	0.00	0.00	0.00	0.90	0.00	0.00	0.00	0.00	0.00	0.00
Cr_2O_3	0.00	0.00	2.58	0.00	0.00	0.00	0.00	0.00	0.00	0.00	0.00
Cations	O = 4	O = 6	O = 4	O = 4	O = 6	O = 4	O = 6		O = 4	O = 6	O = 4
Si	1.002	1.951	0.047	1.021	1.918	1.009	1.994		1.036	1.968	0.137
Al	-	0.210	0.028	-	0.135	-	-		-	-	-
Ca	0.005	0.819	-	-	0.886	-	0.855		-	0.965	-
Mg	1.706	0.825	0.124	1.591	0.851	1.433	0.971		1.017	0.852	-
Fe^{2+}	0.279	0.137	0.853	0.363	0.174	0.548	0.186		0.900	0.247	0.932
Fe^{3+}	-	-	1.855	-	-	-	-		-	-	1.863
Mn	0.004	0.003	-	0.004	-	-	-		0.012	-	-
Ni	0.002	-	-	-	-	-	-		-	-	-
Ti	-	-	-	-	0.025	-	-		-	-	-
Cr	-	-	0.071	-	-	-	-		-	-	-
Mole Percent											
Ca	0.3	45.9		0.0	46.4	0.0	42.5		0.0	46.7	
Mg	85.5	46.2		81.2	44.5	72.3	48.3		52.7	41.3	
Fe	14.0	7.7		18.6	9.1	27.7	9.2		46.7	12.0	
Mn	0.2	0.2		0.2	0.0	0.0	0.0		0.7	0.0	
Mg/(Mg+Fe)	0.860	0.858		0.814	0.830	0.723	0.839		0.531	0.775	

a Analyses have been calculated assuming total oxides = 100 wt. % and without any corrections for possible absorption or fluorescence effects, which are considered to be negligible in the ultrathin specimens used.
b Pyroxene inclusion assumed to be part of a symplectite, but see text.
c All Fe *given as* FeO, *but proportioned into* Fe^{2+} *and* Fe^{3+} *in the recalculated spinel analyses.*

Table 2. (continued)

4310 (Skaergaard)			4308 (Skaergaard)[e]		4472 (Skaergaard)			RPT (Rockport)[g]		
olivine	augite	spinel	olivine	augite	olivine	augite	spinel	olivine	spinel	
32.72	50.28	0.20	31.93	50.64	29.59	46.93	0.23	29.47	0.75	SiO_2
0.00	0.76	2.67	0.00	0.92	0.00[f]	0.00	2.83	0.00	0.00	Al_2O_3
0.15	16.55	0.00	0.26	17.26	0.24[f]	19.34	0.00	0.00	0.00	CaO
15.44	11.29	0.00	11.71	11.51	0.24[f]	0.17	0.00	0.00	0.00	MgO
50.80	19.41	73.85	55.39	19.61	68.72	32.15	88.60	68.14	93.94	FeO[a]
0.67	0.36	0.23	0.00	0.36	1.02	0.77	0.21	3.05	0.00	MnO
0.00	0.00	0.00	0.00	0.00	0.00	0.00	0.00	0.00	0.00	NiO
0.00	0.73	20.85	0.70	0.65	0.00	0.00	4.47	0.00	0.00	TiO_2
n.a.	n.a.	n.a.	n.a.	n.a.	n.a.	n.a.	n.a.	n.a.	0.00	Cr_2O_3
99.77	99.37	97.80	100.00	100.96	99.81	99.40	96.34	100.67	94.68	Total
O = 4	O = 6	O = 4	O = 4	O = 6	O = 4	O = 6	O = 4	O = 4	O = 4	Cations
0.995	1.958	0.009	0.994	1.945	1.002	1.978	0.008	0.995	0.028	Si
-	0.035	0.144	-	0.042	-	-	0.121	-	-	Al
0.005	0.691	-	0.009	0.711	0.009	0.875	-	-	-	Ca
0.700	0.656	-	0.544	0.659	0.013	0.012	-	-	-	Mg
1.291	0.632	0.983	1.442	0.630	1.947	1.133	0.929	1.924	0.986	Fe^{2+}
-	-	1.840	-	-	-	-	1.749	-	1.972	Fe^{3+}
0.018	0.012	0.009	-	0.012	0.030	0.028	0.006	0.087	-	Mn
-	-	-	-	-	-	-	-	-	-	Ni
-	0.022	0.007	0.019	0.019	-	-	0.122	-	-	Ti
-	-	-	-	-	-	-	-	-	-	Cr
0.2	34.7		0.5	35.3	0.5	42.7		0.0		Ca
34.8	32.9		27.3	32.8	0.7	0.6		0.0		Mg
64.1	31.7		72.3	31.3	97.4	55.3		95.7		Fe
0.9	0.6		0.0	0.6	1.5	1.4		4.3		Mn
0.352	0.509		0.274	0.511	0.007	0.010		0.000		

d Small grains often enclosed by olivine. *e The only oxide present in the sample analysed was ilmenite.*
f Variable CaO and MgO contents which are attributed to high symplectite densities.
g Coexisting pyroxene is ferrosilite

Table 3. (continued)

4310 (Skaergaard)[d]		4308 (Skaergaard)			4472 (Skaergaard)			RPT (Rockport)			
olivine	augite	olivine	augite	spinel	olivine	augite	spinel	olivine	augite	spinel	
32.61	49.59	32.47	46.78	12.03	29.58	46.57	1.77	29.12	47.10	2.55	SiO_2
0.00	1.37	0.19	1.74	0.72	0.00	1.11	0.00	0.00	0.70	0.00	Al_2O_3
0.00	21.00	0.00	22.15	4.86	0.00	19.38	0.00	0.00	19.06	0.00	CaO
13.98	10.94	11.89	10.00	2.86	1.10	1.56	0.00	0.00	0.00	0.00	MgO
52.60	16.18	54.66	19.32	79.53	67.59	31.38	98.23	67.34	31.81	97.45	FeO[c]
0.80	0.21	0.79	0.00	0.00	1.73	0.00	0.00	3.24	1.33	0.00	MnO
0.00	0.00	0.00	0.00	0.00	0.00	0.00	0.00	0.00	0.00	0.00	NiO
0.00	0.71	0.00	0.00	0.00	0.00	0.00	0.00	0.00	0.00	0.00	TiO_2
0.00	0.00	0.00	0.00	0.00	0.00	0.00	0.00	0.00	0.00	0.00	Cr_2O_3
O = 4	O = 6	O = 4	O = 6	O = 4[e]	O = 4	O = 6	O = 4	O = 4	O = 6	O = 4	Cations
0.998	1.917	1.004	1.853	-	0.996	1.934	0.062	0.991	1.968	0.090	Si
-	0.062	0.007	0.081	0.019	-	0.054	-	-	0.034	-	Al
-	0.870	-	0.940	-	-	0.863	-	-	0.854	-	Ca
0.638	0.631	0.548	0.591	0.003	0.055	0.097	-	-	-	-	Mg
1.346	0.523	1.413	0.640	0.997	1.903	1.090	0.969	1.925	1.111	0.955	Fe^{2+}
-	-	-	-	1.981	-	-	1.938	-	-	1.910	Fe^{3+}
0.021	0.007	0.021	-	-	0.049	-	-	0.093	0.047	-	Mn
-	-	-	-	-	-	-	-	-	-	-	Ni
-	0.021	-	-	-	-	-	-	-	-	-	Ti
-	-	-	-	-	-	-	-	-	-	-	Cr
0.0	42.8	0.0	43.3		0.0	42.1		0.0	42.5		Ca
31.8	31.1	27.7	27.2		2.7	4.7		0.0	0.0		Mg
67.1	25.8	71.3	29.5		94.8	53.2		95.4	55.6		Fe
1.0	0.3	1.0	0.0		2.5	0.0		4.6	1.9		Mn
0.322	0.547	0.280	0.480		0.028	0.007		0.000	0.000		

d The magnetite in this sample was removed during ion thinning (see text).
e Magnetite analysis has been recalculated assuming all Si is contamination from augite (85%) and olivine (15%). The other elements have been adjusted proportionately.

Table 4. EMMA analyses of pyroxene along a single symplectite from specimen 4308

	Weight percent oxides			
SiO_2	40.5	42.7	45.2	46.8
Al_2O_3	9.9	13.4	2.8	1.7
CaO	8.2	12.8	22.0	22.2
Na_2O	0.0	1.9	0.0	0.0
MgO	12.5	11.4	9.5	10.0
FeO	28.9	17.7	20.4	19.3
	Cations for O = 6			
Si	1.62	1.64	1.81	1.85
Al	0.47	0.61	0.13	0.08
Ca	0.35	0.53	0.94	0.94
Na	0.00	0.14	0.00	0.00
Mg	0.75	0.65	0.57	0.59
Fe	0.97	0.57	0.68	0.64
Mg/(Mg+Fe)	0.44	0.54	0.45	0.48

First analysis is at one end of the symplectite, second and subsequent analyses are progressively further along it. All four analyses are slightly contaminated by olivine, which causes the cation totals to be about three per cent too high.

ally similar, $\langle 010\rangle_{ol}$ and $\langle 013\rangle_{ol}$ are not identical and it is not unexpected that symplectites formed along the two directional sets exhibit differences.

The absence of or, at best, poor structural orientation between host fayalite and the symplectites, apparently, on $(001)_{ol}$ could be because they have grown on slip planes with the host structure having had little influence

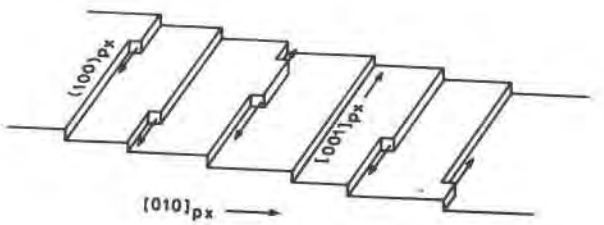

Fig. 4. A schematic illustration of the possible development of growth ledges in pyroxene. This interpretation requires only a few unit cells to be involved in the transformation of olivine to pyroxene at any given locality.

on their development. (Planar (001) precipitate complexes emanating from [001] dislocations have been described by Kohlstedt and Vander Sande (1975) in naturally reheated olivines from Alaska, however, these were oriented.) Despite the lack of a structural relationship with their host, the symplectites in this specimen branch in a fashion similar to those in other samples, while the "embryo" symplectites (Fig. 1f) have an appearance similar to the suggested early growth stage in Figure 6a. This may indicate that some directions, such as ⟨112⟩, are strongly preferred magnetite growth directions, or more likely it is a natural result of two phases precipitating penecontemporaneously. Material not required in one phase is ejected from it to be incorporated into the second phase, which in turn transfers those cations not compatible with its structure to the first phase, *etc*. The branching seen in symplectites is the consequence of minimizing the exchange distances. In more usual circumstances topotaxic control restricts this branching to directions which favor the fastest growth.

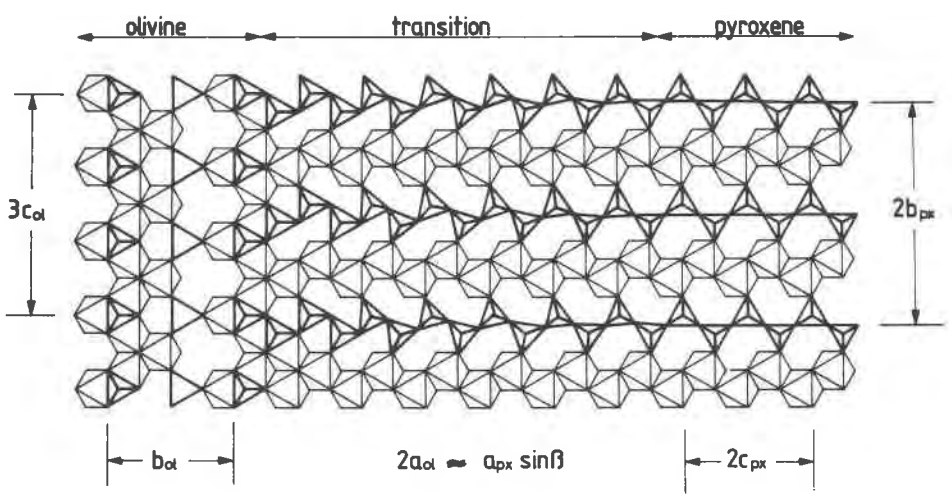

Fig. 5. A partial projection on the common (100) plane of olivine and pyroxene in the orientations obtained from the diffraction pattern in Fig. 3a. The central part of the diagram shows a possible transformation scheme.

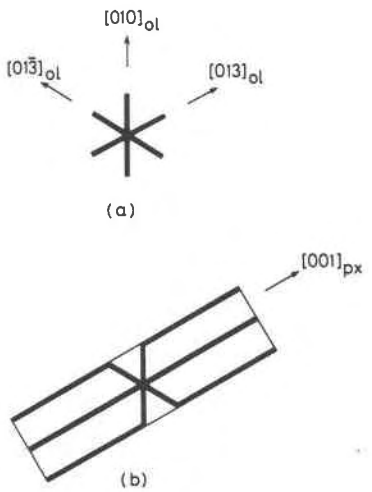

Fig. 6. A possible symplectite development scheme. (a) Nucleation and growth of magnetite along its six equivalent ⟨112⟩ directions on a (111) face. (b) Pyroxene precipitates and grows preferentially in one of its three possible orientations. The pyroxene is assumed to grow fastest along its chain direction, taken to be parallel to $[013]_{ol}$ in this example. Cooperative growth between pyroxene and magnetite then ensures that the $\langle 112\rangle_{mt}$ parallel to $[013]_{ol}$ develop faster than the other $\langle 112\rangle_{mt}$ giving the elongated shape commonly observed.

Comparison of microprobe and analytical electron microscope results (Tables 2 and 3) show that, when present, primary augite crystals coexisting with olivines have chemical compositions similar to those of the pyroxene phases in the symplectites. Variations in proportions of Mg to Fe in the two pyroxene types is not systematic and is usually small, though the symplectite pyroxenes tend to be less magnesian than the coexisting primary grains. Al contents are usually higher in the symplectite pyroxene than in the coexisting augite crystals, while variations in the wollastonite components are greater in the different coexisting primary grains (35–48 mole%) than in symplectic augites (42–47%). Though generally the composition of symplectite magnetite is similar to that of the coexisting grains of primary spinel, the correspondence is not as good as for the pyroxenes and for specimen 199 the difference is extreme. It is, however, significant that in this Rhum specimen the high Cr and Al contents of the primary spinel crystals are reflected, to a lesser degree, in the symplectite. In fact the symplectite spinel in this sample is the only one in which Cr was detected. It also contains the largest amount of Al; the slightly higher measured quantity of Al in 4308 is partly contamination from the adjacent pyroxene. These general compositional similarities were not expected as the primary and exsolved phases were formed from different bulk compositions (melt and host olivine) and at different temperatures and pressures.

Ratios of Mg/(Mg+Fe) in symplectic pyroxene have been plotted against those of the host olivine in Figure 7 from the EMMA-4 data given in Table 3. Also plotted on this figure are the augite compositions in symplectites reported by Gooley *et al.* (1974) and Arai (1978) which do not fit the general trend of those reported in this study. This may be related to that fact that in these two symplectites the spinel phase is chromite and not magnetite.

Previous ideas of symplectite formation

Several hypotheses have been put forward to explain the occurrence of these intergrowths. Judd (1885) attributed them to secondary products filling negative crystals. The irregularly shaped ones resulting from incomplete filling of these cavities while those with straight edges are completely filled negative crystals. The dendritic structure "is partially determined by crystalline forces" controlling "the distribution of these products of decomposition". There is, however, no evidence for negative crystals, which are unlikely to occur in minerals formed at pressures of about a kilobar. Judd deduced the presence of negative crystals from the rectangular shapes of many symplectites, the true nature of which he had not appreciated (that is, they are artificially introduced by sectioning through the intergrowths as, for example, B in Fig. 1b). It would, in any case, be difficult to account for either the overall shape of such negative crystals, which would be several hundred times longer in the *b* and *c* directions than along the *a*-axis of olivine, or for some of their detailed profiles (and the way in which they would have to be infilled) such as that in Figure 2c.

Putnis (1979) has interpreted these symplectites as being formed by oxidation with subsequent cellular decomposition to an eutectoidal intergrowth of magnetite and pyroxene. However, since these type A symplectites are not found near the edges of olivine crystals—a zone in which oxidation would be expected to occur at an early stage—this seems an unlikely mechanism. Nor can this mechanism easily account for Figure 1b, which shows two generations of symplectites; the second being absent in the vicinity of the first. A further difficulty is that the chemical evidence given in Table 3 is not compatible with cellular decomposition being involved. In essence, cellular decomposition is a mechanism whereby daughter phases can grow rapidly by eliminating the necessity for long range diffusion, such as would be required if they segregated into discrete grains. As can be seen from Table 3, the pyroxene in these symplectites acts as a depository for those elements, such as Ca and Al, which are not entirely compatible with the ferro-magnesian olivine structure. Consequently considerable long range diffusion has occurred. These symplectites have, therefore, grown slowly enough for the "incompatible" cations to diffuse to them at about the time pyroxene was

being formed. The Ca ions, at least, cannot be a subsequent replacement, since then concentration gradients with low Ca in the pyroxene at the edge of a symplectite increasing to higher values further in (Table 4) would not be found. Unlike the cellular intergrowths found in metals, type A symplectites are not, therefore, a result of rapid growth conditions.

In their discussion on the origin of type A and B symplectites, Bell *et al.* (1975) suggested two alternative hypotheses: "solid-state breakdown and reaction of pre-existing chrome garnet crystals and host olivine" (the spinel phase in their symplectites was chromite) and "solid-state diffusion and precipitation of minor elements out of olivine". The garnet hypotheses is unacceptable for at least some of the olivines in this report. In particular the Skaergaard intrusion formed at a shallow depth and differentiated as a closed system. Olivines formed in the Upper Zone, such as those used in this work, are most unlikely to have ever contained any garnet. A reservation put forward by Bell *et al.* (1975), for their model of solid-state diffusion and precipitation of minor elements, was the unlikelihood of three different phases (spinel, orthopyroxene and clinopyroxene) precipitating simultaneously from the host phase. The results presented here suggest that this need not have happened. Their spinel–two pyroxene assemblages could start as chromite-augite intergrowths with the clinopyroxene subsequently becoming an orthopyroxene because of either exhaustion of Ca before symplectic formation was complete, or these symplectites continued growing at temperatures too low for effective Ca diffusion. Of the various hypotheses considered the diffusion and precipitation seems the most likely.

Symplectite formation by exsolution

Although large trivalent cations can form stable olivine structures (*e.g.*, $LiScSiO_4$, Ito, 1977) small ones do not, seeming to prefer four-fold coordination and to form framework structures with Si, as for example in the various $LiAlSiO_4$ polymorphs. Trivalent cations of intermediate size, such as Fe and Cr, may be stable (in small amounts at least) in olivine at high temperatures. They would, however, almost certainly be expelled on cooling, when contraction of the crystal brings the 3+ cations too close to Si^{4+} ions and the charge repulsion between them becomes too great. Assuming the trivalent cation to be present in a hypothetical component such as $Fe^{3+}_{4/3}SiO_4$ (or the $Cr^{3+}_{4/3}SiO_4$ suggested by Arai, 1978) the breakdown can be represented as a reaction between this and a fayalite component producing spinel and silica:

$$3R^{3+}_{4/3}SiO_4 + Fe^{2+}_2SiO_4 \rightarrow 2R^{3+}_2Fe^{2+}O_4 + 4SiO_2 \quad (1)$$

where R = Fe, Cr. The silica in turn reacts with more olivine to form the pyroxene:

$$4SiO_2 + 4X_2SiO_4 \rightarrow 4X_2Si_2O_6 \quad (2)$$

X = Ca, Mg, Fe. Overall the reaction may be written:

$$3R^{3+}_{4/3}SiO_4 + Fe^{2+}_2SiO_4 + 4X_2SiO_4 \rightarrow 2R^{3+}_2Fe^{2+}O_4 + 4X_2Si_2O_6 \quad (3)$$

Whether the pyroxene formed in this way is augite or hypersthene will depend on the amount of Ca present and, possibly, the temperature of formation. Equation (3) indicates that for clinopyroxene to be formed a Ca^{2+} ion is required for every trivalent cation involved in the formation of spinel. (More complex models predicting different ratios of pyroxene to spinel are possible if some of the Fe^{3+} replaces Si.)

An objection to the scheme given by Equations (1) and (2) is that since quartz and fayalitic olivines are compatible phases, Reaction (2) would not occur at the Fe-rich end of the range. Nor are these reactions strictly compatible with the scheme illustrated in Figure 5. In practice the reaction will proceed by cation diffusion and SiO_2 will not be formed at any stage. Assuming that the reaction is initiated by trivalent cations being expelled from the olivine structure a possible cation exchange model which may also be summarized by Equation(3) is:

$$2XFeSiO_4 + 4R^{3+} \rightarrow 2FeR^{3+}_2O_4 + 2Si^{4+} + 2X^{2+} \quad (4)$$

where X = Ca, Mg, Fe and R = Fe, Cr as before.

$$3X_2SiO_4 + Si^{4+} \rightarrow 2X_2Si_2O_6 + 2X^{2+} \quad (5)$$

and

$$3R^{3+}_{4/3}SiO_4 + 4X^{2+} + Si^{4+} \rightarrow 2X_2Si_2O_6 + 4R^{3+} \quad (6)$$

Equations (4) to (6) indicate cross-diffusional movements (similar to those forming cellular intergrowths in metals) in which trivalent cations leave pyroxene-rich areas for spinel-enriched zones, while divalent and Si^{4+} cations move in the reverse direction. Though, obviously, there has to be an initial stage of long-range diffusion to bring Fe^{3+}, Cr^{3+} (and Al^{3+}, Ca^{2+}) to the reaction site, it is this complex, short-range diffusion that is responsible for the dendritic structure observed. (While the continuing long-range diffusion will determine the rate of symplectite formation.) Although, morphologically, symplectites resemble the products of cellular decomposition, because they are, in part, formed by a similar diffusion mechanism, there are some differences. For example, cellular decomposition, *e.g.*, the formation of pearlite in the Fe–C system, occurs only at, or near, a eutectoidal composition. This contrasts with symplectites which form over at least 90% of the olivine compositional range (Fig. 7). Further, cellular decomposition nucleates at the edges of a grain and grows into the adjacent crystals. There is, therefore, no structural orientation between the products formed by cellular decomposition and the host matrix in which they grow. Again this is different from the symplectites. Also, as noted above, long range diffusion is essential for symplectite formation, while "classical" cellular decomposition is regarded as a mechanism (for the rapid

formation of two phases from a single phase) which avoids the need for long range diffusion. Thus, if there is a relationship between symplectic formation and cellular decomposition, it is not a straightforward one, as both have features the other lacks.

The study of Kohlstedt and Vander Sande (1975) was of olivines from lherzolites "which were altered during or following a lava flow". The precipitate complexes they described, which have some morphological features of symplectites, formed as a result of thermal metamorphism (as apparently did at least some of the symplectites in the Rockport fayalite). Since these precipitate complexes contain a silica phase (tridymite) as well as orthopyroxene and magnetite, they may represent incomplete symplectic development as described by Equations (1) and (2). This could imply that the symplectite formation given by Equations (1) and (2) represents a faster mechanism than that of the diffusion model (Equations (4) to (6) though this latter model is probably the one by which symplectites usually form. The small amount of hematite found in their precipitate complexes could be either a precursor phase of magnetite formation or, a subsequent oxidation of it. While the pyroxene phase is orthorhombic either because insufficient Ca was available for augite formation or because conditions were unfavorable for it to diffuse to the precipitate sites in any quantity (*e.g.*, a high enough temperature for a sufficient length of time). Unfavorable conditions might also account for the orthopyroxene observed in one of the symplectites of the Rockport fayalite (Fig. 2f). The orthopyroxene may have been the first phase to precipitate along with the magnetite. At higher temperatures, when Ca was able to diffuse at a reasonable rate, the pyroxene type changed to the monoclinic form with, possibly, some partial conversion of the orthopyroxene to clinopyroxene.

If type A symplectites do form in accordance with Equation (3) then they should contain about three volumes of pyroxene for every volume of spinel. On this basis, symplectites occupying two volume percent of the host (the maximum normally to be expected) represent 0.45 wt. % Fe_2O_3 (or Cr_2O_3) and 0.3 wt. % CaO in the olivine analysis. Micrographs, such as those in Figures 1 and 2 indicate a pyroxene:magnetite ratio that is lower than this. Values obtained from micrographs can be misleading because of the strong absorption of photons and electrons by magnetite, which therefore tends to mask any pyroxene in direct line of sight. For example, in the section through a symplectite shown in Fig. 2a there is more pyroxene than magnetite visible, but had it been viewed along [100] instead this same section would have appeared to contain almost equal amounts of magnetite and pyroxene. That in Figure 2e gives an erroneous impression in the orientation shown, since pyroxene is present along the whole of the dislocated interfaces. A further complication is determining volume ratios from what, especially in electron micrographs, are essentially two-dimentional views. However, if it is assumed that the ratio of pyroxene to magnetite is uniform in all directions, then since volume (V) is proportional to the cube of a linear dimension (X) and area (A) is proportional to the square of X, then $A \propto X^2 \propto V^{2/3}$. Thus sections through a symplectite should, typically, contain $3^{2/3}$ (~2.08) times more pyroxene than magnetite, which is about the average ratio observed in electron micrographs (such as Fig. 2). Although it may thus be argued that the evidence for the ratio of symplectic phases is not inconsistent with the predicted value, there is need for more work on this aspect since it places an important constraint on formation models. (Bell *et al.*, 1975 thought the spinel in their type A symplectites occupied about $\frac{1}{3}$–$\frac{1}{2}$ the volume).

A tentative scheme of symplectite formation

One possible explanation of the variation in Mg/(Mg+Fe) ratios between exsolved augite and olivine host is presented in Figure 8. The phase diagram at the top of this figure is the one atmosphere diopside-hedenbergite binary simplified by omitting the complications of wollastonite solid solutions at the iron-rich end. The line PQ represents a theoretical limit of thermal stability of Fe^{3+} in olivine of a given Mg/(Mg+Fe) composition. For simplicity and because nothing is known of its actual shape it has been drawn as a straight line and its interception with the augite solidus and liquidus has been chosen to give the best fit for the data given in Figure 7.

The diagram in the lower part of Figure 8 is derived as follows. At high magnesian compositions, such as A, ferric iron is stable in olivine to below the augite solidus and the transformation of olivine to magnetite and pyroxene is a solid-state reaction. Assuming that Ca replaces Mg and Fe in the ratio of their relative abundances (for composition A this is 19:1) the resulting augite will have a Mg/Fe composition the same as the original olivine. The extra iron removed from the olivine to form the magnetite increases the forsterite content of the olivine, but for all practical purposes initial and final olivine compositions are the same as only about one per cent of the crystal is involved. The result is the 45° slope for compositions between pure forsterite and that of B. For olivines more fayalitic than composition B the transformation occurs above the augite solidus. For composition C this happens when olivine has cooled to c_1. If the temperature then remains constant an augite of composition c is produced and an iron-enriched liquid which aids the formation of magnetite. Removal of magnetite, which (because its melting point is well above that of diopside) solidifies, causes Mg enrichment of the residual liquid and consequently more augite of composition c is precipitated. A process which continues until all the liquid has been used up, resulting in a pyroxene with a higher Mg/(Mg+Fe) ratio than that of the original olivine. Since for compositions more magnesian than Fo_{40} there is insufficient Fe available for the formation of magnetite if the liquid bulk

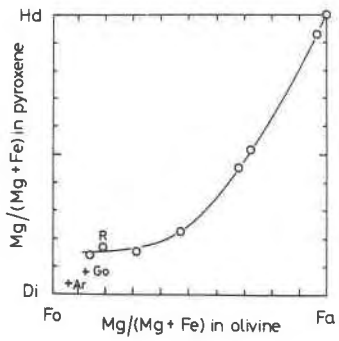

Fig. 7. Plot of Mg/(Mg+Fe) ratios of symplectite pyroxene against those of the host olivine. R is the pyroxene composition of RH9 which may not be from a symplectite. Ar and Go are from Arai (1978) and Gooley *et al.* (1974), respectively. The symplectites reported in those two studies differ from those forming the main trend in this diagram by having chromite as the coexisting spinel phase.

composition is the same as the olivine, there will also be a reaction between this liquid and the olivine to enrich the melt with Fe. Thus, as for high forsterite compositions, there is an undetectable decrease in fayalite content of the host olivine. For the fayalitic compositions beyond D the ferric iron is exsolved above the augite liquidus. Removal of magnetite results in a Mg enriched melt of augite. Olivine of composition E, for example, will on cooling below PQ transform to magnetite and a pyroxene melt with a Mg/(Mg+Fe) ratio of e_1. Assuming that for this composition no reaction occurs between the pyroxene melt and solid olivine, other than indiscriminate Mg, Fe replacement by Ca, this melt will eventually reach the augite liquidus and form a pyroxene with a composition of e_2. Normal equilibrium cooling then follows and a pyroxene of composition e results, thus causing the steep profile in the lower diagram of Figure 8 for compositions between D and pure fayalite. For compositions between D and Fo_{40}, unlike that of E, reaction between liquid and olivine will occur to produce the necessary Fe enrichment for magnetite formation resulting in the discontinuity at Fo_{40}. (It would be desirable to examine symplectites in olivines near this compositional point as a test of this hypothesis.)

The stippled lines in the lower diagram of Figure 8 show the deviations, from the main diagram, which would occur if the line PQ is redrawn at a higher level for a nonferric ion. It represents the possible effect the smaller Cr^{3+} has on exsolved pyroxene compositions. However, the points A and G in this diagram could equally well be accommodated in the proposed exsolution scheme by postulating for high Mg compositions that the trend has a slope of less than 45° with respect to the abscissa. This could result, for example, from the removal of Fe from the pyroxene to help form magnetite at these high forsterite contents. Further work on chromite symplectites will be required to determine which, if either, of these explanations is correct.

Some supporting evidence for the suggested temperature of symplectic formation may be obtained form heating experiments. Roedder and Weiblen (1971) heated lunar olivines, with a composition apparently, of about Fo_{78}, in vacuo to 1219°C without affecting the enclosed type A symplectites. This can be interpreted either, that the formation temperature of these symplectites was higher than this or, that the run duration (three hours) was too short to have any effect. However, a one hour run with an olivine from the same sample (12018) by Bell *et*

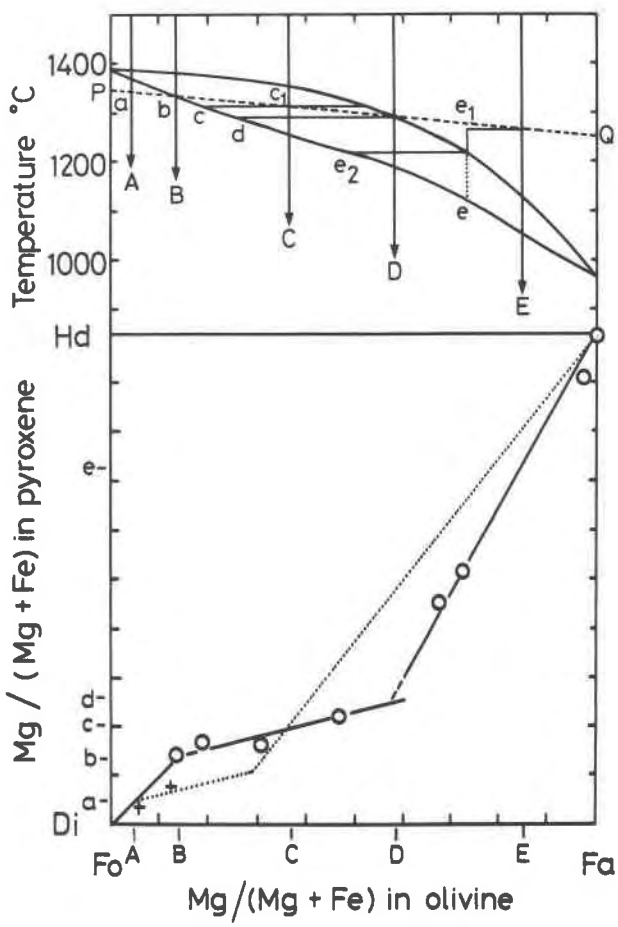

Fig. 8. An interpretation of the Mg:Fe ratios in olivine and exsolved pyroxene. Top is the one atmosphere phase diagram of the diopside-hedenbergite join with the complications of wollastonite solid solution omitted for clarity. PQ represents the temperatures at which Fe^{3+} becomes unstable in olivine of any given composition. a–e are the compositions of the pyroxenes exsolved from the olivines of compositions A–E. Lower diagram shows the resulting compositional relation between olivine and symplectite pyroxene (solid line). The dotted line shows the deviation to be expected if the breakdown occurs at slightly higher temperature with a non ferric cation, such as Cr^{3+}.

al. (1975) at 1300° showed some recrystallization. This is approximately, though a little below, the temperature at which symplectites in olivines of this composition would be predicted to form by the model presented here. However, it is also above the solidus for augites of this composition.

The unusual combinations of factors evoked to explain this type of exsolution would make type A symplectites a rare occurrence and, as far as is known, they are not found in any minerals other than olivines.

Acknowledgments

Samples of speciments 199, 4308, 4310, 4472 and 9898 were made available for this work by W. J. Wadsworth. The Rockport fayalite was supplied by P. E. Champness who together with J. Zussman read earlier versions of this manuscript and made many helpful comments. I am very grateful to all three for their help and also to I. Brough and G. Cliff for assistance with the electron microscopy. Financial support for this work was provided by a grant from the NERC.

References

Ambler, E. P. and Ashley, P. M. (1977) Vermicular orthopyroxene–magnetite symplectites from the Wateranga Layered mafic intrusion, Queensland, Australia. Lithos, 10, 163–172.

Arai, S. (1978) Chromian spinel lamellae in olivine from the Iwanai-Dake peridotite mass, Hokkaido, Japan. Earth and Planetary Science Letters. 39, 267–273.

Bell, P. M., Mao, H. K., Roedder, E. and Weiblen, P. W. (1975) The problem of the origin of symplectites in olivine-bearing lunar rocks. Proceedings of the Sixth Lunar Science Conference, 1, 231–248.

Champness, P. E. and Lorimer, G. W. (1974). A direct lattice-resolution study of precipitation (exsolution) in orthopyroxene. Philosophical Magazine, 30, 357–365.

Gooley, R., Brett, R., Warner, J. and Smyth, J. R. (1974) A lunar rock of deep crustal origin: sample 76535. Geochimica et Cosmochimica Acta, 38, 1329–1339.

Harker, A. (1954) Petrology for Students, (eighth edition). Cambridge University Press, Cambridge, U.K.

Hatch, F. H., Wells, A. K. and Wells, M. K. (1972) Petrology of the Igneous Rocks, (thirteenth edition). Thomas Murby and Co., London.

Ito, J. (1977) Crystal synthesis of a new olivine, $LiScSiO_4$. American Mineralogist, 62, 357–361.

Judd, J. W. (1885) On the Tertiary and older peridotites of Scotland. Quarterly Journal of the Geological Society of London, 41, 354–418.

Kohlstedt, D. L. and Vander Sande, J. B. (1975) An electron microscopy study of naturally occurring oxidation produced precipitates in iron-bearing olivines. Contributions to Mineralogy and Petrology, 53, 13–24.

Penfield, S. L. and Forbes, E. H. (1896) Fayalite from Rockport, Mass., and on the optical properties of the chrysolite–fayalite group and of monticellite. American Journal of Science, 151, 129–135.

Putnis, A. (1979) Electron petrography of high-temperature oxidation in olivine from the Rhum layered Intrusion. Mineralogical Magazine, 43, 293–296.

Roedder, E. and Weiblen, P. W. (1971) Petrology of silicate melt inclusions, Apollo 11 and Apollo 12, and terrestrial equivalents. Proceedings of the Second Lunar Science Conference, 1, 507–528.

Smith, P. P. K. (1979) The identification of single-domain titanomagnetite particles by means of transmission electron microscopy. Canadian Journal of Earth Sciences, 16, 375–379.

Zirkel, F. (1871) Geologische Skizzen von der Westkuste Schottlands. Zeitschrift der deutschen Geologischen Gesellschaft, 23, 1–124.

Manuscript received, July 29, 1981;
accepted for publication, May 26, 1983.